Environment International 190 (2024) 108944

Contents lists available at ScienceDirect

Environment International

journal homepage: www.elsevier.com/locate/envint

Full length article

Aquatic toxicity and chemical fate of diluted bitumen spills in freshwater under natural weathering

S.L.J. Hepditch [a,d,e], J.M. Gutierrez-Villagomez [a], T.A. To [a], E. Larocque [a], Q. Xin [b], N. Heshka [b], I. Vander Meulen [c], J.V. Headley [c], H.D. Dettman [b], G. Triffault-Bouchet [d], J.M.E. Ahad [e], V.S. Langlois [a,*]

[a] Institut national de la recherche scientifique (INRS), 490 rue de la Couronne, Québec City, QC G1K 9A9, Canada
[b] Natural Resources Canada (NRCan), CanmetENERGY, 1 Oil Patch Drive, Devon, AB T9G 1A8, Canada
[c] Environment and Climate Change Canada, Watershed Hydrology and Ecology Research Division, National Hydrology Research Center, 11 Innovation Boulevard, Saskatoon, Saskatchewan S7N 3H5, Canada
[d] Centre d'expertise en analyse environnementale du Québec, ministère de l'Environnement et de la lutte contre les changements climatiques, de la faune et des forêts (MELCCFP), Québec City, QC H7C 2M7, Canada
[e] Geological Survey of Canada, Natural Resources Canada (NRCan), Québec City, QC G1K 9A9, Canada

ARTICLE INFO

Handling Editor: Adrian Covaci

Keywords:
Fathead minnow
Dilbit
Embryotoxicity
Oil toxicity
Oil behaviour

ABSTRACT

Increasing global demands for oils are fueling the production of diluted bitumen (DB) from Canada's oil sands region. More weathered than conventional crude (CC) oils, Alberta bitumen is often diluted with lighter petroleum oils to reduce density and viscosity to meet pipeline specifications for transportation. Being a heavy oil product that is transported in large volumes across Canada and the USA, there has been interest to compare its behavior and toxicity characteristics when spilled to those of CC. To determine the influence of environmental weathering upon DB following a freshwater spill, we conducted separate controlled spills of Cold Lake Blend DB and Mixed Sweet Blend light CC oil in a mesocosm spill-tank system at 24 °C with wave-action for 56 days. DB-contaminated waters remained acutely lethal for a period of 14 days to early life stage fathead minnows (*Pimephales promelas*) exposed during embryologic development, while CC was lethal for 1 day. However, concentrations of mono- and polycyclic aromatic compounds, often claimed to be principally responsible for the acute and chronic toxicity of crude oils, were consistently higher in CC water compared to DB. Elevated aromatic concentrations in CC water correlated with higher prevalences of developmental malformations, reduced heart and growth rates, and impacts on the aryl hydrocarbon receptor pathway. Organic acids were measured over the course of the studies and O_2 containing naphthenic acids were present at greater relative abundances in DB- compared to CC-contaminated water, with their attenuation correlating with reduced acute and sublethal toxicity. Furthermore, organic acid degradation products accumulated with time and likely contributed to the consistently sublethal toxicity of the weathered oils throughout the experiment. Improved characterization of the fractions including organic acids and those organic compounds found within the unresolved complex mixture of fresh and weathered crude oils is necessary to adequately understand and prepare for the risks that accidental petroleum spills pose to aquatic resources.

1. Introduction

Bitumen is an extra heavy oil defined by its immobility in source reservoirs (Speight, 2019). Western Canada contains the world's largest deposit of extractable bitumen and production has continued to increase in response to international demand for oil (CER, 2022; Hein, 2017). Bitumen is a high density, viscous oil due to prolonged periods of weathering in the reservoir that has removed the more labile constituents and concentrated the larger, more polar compounds. As its density and viscosity are too high to meet pipeline specifications for transportation as produced, bitumen is diluted with naphtha-based condensates to form the product called diluted bitumen (DB). However, being a heavy oil product, DB still has higher density, viscosity and abundance of high molecular weight (HMW) compounds compared to conventional

* Corresponding author at: Institut national de la recherche scientifique (INRS), Centre Eau Terre Environnement, Québec, QC G1K 9A9, Canada.
E-mail address: valerie.langlois@inrs.ca (V.S. Langlois).

https://doi.org/10.1016/j.envint.2024.108944
Received 15 April 2024; Received in revised form 2 August 2024; Accepted 6 August 2024
Available online 8 August 2024

crude (CC; *i.e.,* Hounjet et al., 2023; Saborimanesh et al., 2023). DB spilled into freshwater has been found to float for days to weeks after being spilled into fresh water. However, if not recovered, like other types of petroleum products, portions of the oil will become submerged or sink depending upon the conditions of the spill (Stoyanovich et al., 2021, 2023; Xin et al., 2023, 2024). This post-spill behavior was observed during the accidental spill event in the Kalamazoo River (Michigan, USA) in 2010. Despite high recovery rates for the diluted bitumen floating at the start of the response operations, loss of the lower molecular weight fractions of the dilbit blend and interaction with shorelines and sediments resulted in submergence in the water as the response progressed, resulting in extensive environmental contamination and remediation efforts (NOAA, 2019). In general there has been much less spill response experience with DB compared to other petroleum products, so questions have been raised regarding how the composition and physical characteristics of DB could influence the transport and fate of potentially toxic compounds in the oil compared to those found for CC oils under the same conditions.

Environmental risks associated with crude oil spills often focus on the aqueous concentrations of mono- and polycyclic aromatic compounds (MACs and PACs, respectively). Although these compounds comprise only a small fraction of crude oils, they are of sufficient water solubility to become bioavailable and are known to induce acute and chronic toxicity to receptor aquatic organisms (NASEM, 2022). These compounds induce a dose-dependent syndrome of toxicity characteristic of petroleum constituents, including acute lethality and chronic, developmental toxicity (Incardona & Scholz, 2017). However, the toxicity of crude oils is also related to the less characterized components within the "unresolved complex mixture" (UCM), which can contain more polar fractions (Meador & Nahrgang, 2019; Melbye et al., 2009; Sørensen et al., 2016). Previous studies characterizing the influence of weathering upon crude oils spilled in water over time have demonstrated an increased production of oxidized organic compounds due to degradation (*i.e.* microbial), which has shown correlations to the sublethal toxicity of these crude oils for periods of up to 35-days (Gutierrez-Villagomez et al., 2024; Heshka et al., 2022; Lara-Jacobo et al., 2021). It is unknown how long these oxidized petroleum constituents may remain as persistent toxicants within contaminated freshwater systems, and direct comparisons between the weathering and subsequent toxicity of DB with CC oils are currently lacking.

Within the current study, we investigated the weathering of a spilled Cold Lake Blend DB and a Mixed Sweet Blend light CC oil for 56 days in warm waters representative of summer conditions (24 °C) with wave-action in a controlled laboratory mesocosm system. The system was filled with North Saskatchewan River water and sediments collected near the city of Edmonton, AB, Canada. Routine water column sampling was conducted to characterize the aromatic fractions and oxidized compounds within the acid extractable organics (AEOs) fraction. Additionally, 7-day fathead minnow (*Pimephales promelas*) embryotoxicity assays were conducted to assess the acute and chronic toxicity of weathered crude oils, with sublethal endpoints including the proportion of developmental malformations, reductions in heart rate and growth, and the activity and expression of CYP1A phase I biotransformation pathways.

2. Methodology

2.1. Microcosm spill system

The spill test was carried out in a 3 m × 1 m × 1.5 m (L×W×H) indoor mesocosm spill-tank (Figure S1), as described previously by Heshka et al. (2022) and Xin et al. (2024). This system held 1,200 L of Saskatchewan River Water collected before treatment from the Edmonton municipal water facility and was maintained at a controlled temperature to simulate summer conditions (24 ± 0.5 ∘C). Waves at an approximative wave height of 10–12 cm were consistently generated using a paddle attached to an external motor for the initial two-day period, followed by a two-day interval with no wave action. This alternating cycle was repeated throughout the duration of the test. The mixing energy applied was tailored to mimic the conditions found in an inland river oxbow, where wave generation typically depends on wind patterns. In cases where the transition from active to inactive wave generation, or vice versa, coincided with a weekend, the respective state was maintained until the following Monday, extending the duration to a third day if necessary. Illumination during testing was provided by LED lights (SafeSite Area Light, Farmingdale, New Jersey, USA; peak wavelength 590 nm, 7300 Lumens, 52 Watts, 100–277 VAC, Cool White 5000 K, clear glass). As LED lights have low or no emissions in the ultraviolet wavelength range (Cosmin and Paul, 2015), it was expected that photo-oxidation contributions to weathering processes in this tank system were also low.

Approximately 10 L of oil was added to the separate spill experiments (9.27 kg of DB and 8.54 kg of CC), with oil–water ratios (1:120 v/v) chosen to maintain an oil thickness of 5 mm on the water surface and enough oil to ensure detection within the water samples collected. Samples of the water-accommodated fraction (WAF) were collected from a spout located 39.5 cm below the floating oil mat within the tank system (water height was 70 cm and the spout was 30.5 cm from the tank bottom). There were negligible differences in measured total organic carbon of waters collected from different locations of similar depth below the floating oil mat within the spill tank (unpublished data), indicating our sampling location was representative of the water accommodated fraction of the 1200 L water column. The durations for both spill tests were 56 days, with water samples being collected on Days 1, 3, 5, 7, 14, 21, 28, 35, 42, 49, and 56. The tank environment allowed for controlled experimentation without the complexities and costs associated with natural spill scenarios, enabling comprehensive analysis of oil behavior and organic compound concentrations in water samples collected throughout the test period.

2.2. Oil and water characterization

Cold Lake DB (produced by *in situ* extraction in the Cold Lake region of Alberta, Canada) and Mixed Sweet Blend light sweet CC oil (benchmark conventionally produced light sweet crude from Western Canada) were obtained courtesy of the Canadian Association of Petroleum Producers from a pipeline in the Edmonton area. Boiling point distributions were measured using high-temperature simulated distillation analyses per the ASTM method D7169-11 (ASTM, 2016) on an Agilent (Santa Clara, CA, USA) gas chromatograph (GC 7800A). Water concentrations of total organic carbon (TOC) were measured according to the American Society for Testing and Materials (ASTM) D7573-09 standard (ASTM, 2009). Chemical analyses of total petroleum hydrocarbons of C_{10}-C_{50} and aromatics were conducted by the center d'expertise en analyse environnementale du Québec (CEAEQ), from the Ministère de l'Environnement, de la Lutte contre les changements climatiques, de la Faune et des Parcs laboratories (QC, Canada) which are accredited by the Standards Council of Canada (ISO/CEI 17025). Total concentrations of MACs, characterized from the volatile organic compounds (VOCs) fraction, and PACs were analyzed by gas chromatography mass spectrometry (GC–MS) in selected ion monitoring mode, and C_{10}–C_{50} concentrations were analyzed by GC-Flame Ionization Detection (GC-FID), all following standardized laboratory protocols (CEAEQ, 2015, 2016a, 2016b). Briefly, VOCs were characterized using a Purge and Trap Concentrator system (Tekmar Stratum Aquatek 100, Teledyne Tekmar, Manson, OH, USA) with a Vocarb 3000 absorbent (Siemens Industry Inc., Munich, Germany), outfitted to a GC–MS (Trace GC Ultra and Trace MS DSQII, Thermo Scientific, Waltham, MA, USA) equipped with a Rtx-VMS column (20 m × 0.18 mm × 1 μm; Restek Co., Centre County, PA, USA). The following GC oven temperature program was used: 35 °C (2 min), increased to 100 °C at 12 °C/min, increased to 230 °C at 30 °C/min (hold 2 min), increased to 240 °C at 0.5 °C /min (hold 2 min). For

C_{10}–C_{50}, water samples were agitated overnight with hexane, with the subsequent organic extracts concentrated via rotary evaporation. C_{10}-C_{50} samples had silica gel added to the organic extract to remove polar compounds, with the resulting hexane sample analyzed for total petroleum hydrocarbons of C_{10}-C_{50} analyzed using an Agilent 6890 GC/FID with an Agilent 7683 autosampler, and Agilent Openlab software was used for system control and data acquisition. A DB-1 column (15 m length ×_0.53 mm diameter, 0.15 μm film thickness) was used for GC separation. The carrier gas was helium at 5.0 mL min^{-1}. The injector and detector temperature were set at 290 and 300 °C, respectively. The oven temperature settings for the TPH analysis ran at 40 °C for 0.25 min, then ramped up at 30 °C min^{-1} to 300 °C for 7 min. For PACs, the organic extract was passed through a chromatographic column packed with fully activated silica. An F1 fraction containing aliphatics was collected in hexane and a subsequent F2 fraction containing aromatics was collected in dichloromethane. The F2 fraction containing aromatics was analyzed individually for PACs using the same GC–MS described above for MAH analysis equipped with a DB-EUPAH column (30 m length ×, 0.25 mm diameter × 0.25 μm film thickness; Agilent, Santa Clara, CA, USA). The following GC oven temperature program was used: 80 °C (1 min), increased to 320 °C at 35 °C/min, increased to 335 °C at 3 °C/min (hold 10 min). Concentrations of 62 VOCs, including benzene, toluene, ethylbenzenes and xylenes (BTEX), and of 86 parent and alkylated PAHs were measured, with the limit of quantification of 1 ng g^{-1} (standards and surrogate standard recovery efficiencies provided in Text S1 and S2).

For quality control and quality assurance purposes, each batch of samples had a method blank analysis to monitor laboratory background levels and each batch contained an analysis of a set of triplicate water samples with observed standard deviations of the mean being less than 15 %. All results were calibrated and quantified using certified calibration standards with a minimum 4-point calibration curve. All samples were injected with 4 μg L^{-1} of internal standard (*m*-terphenyl) or their appropriate recovery (surrogate) standards. For VOCs, recovery of surrogate standards included 1,2-Dichloroethane- d_4 (99 ± 21 % recovery), Toluene-d_8 (100 ± 15 %), 4-Bromofluorobenzene (89 ± 12 %). For PAHs, recovery included 2-Methylnaphthalene-d_{10} (72 ± 18 %), Acenaphthene- d_{10} (80 ± 19 %), Anthracene- d_{10} (93 ± 14 %), Pyrene-d_{10} (89 ± 9 %), Chrysene- d_{10} (92 ± 10 %), Benzo[a]pyrene-d_{10} (85 ± 13 %), Dibenzo[*a,h*]anthracene- d_{14} (89 ± 9 %). All recoveries fell within the acceptable limits of detection.

The acid extractable organics (AEOs) fraction was both semi-quantitatively and qualitatively analyzed under negative ion electrospray ionization with a dual pressure linear ion trap high-resolution mass spectrometer (LTQ Orbitrap Elite, Thermo Fisher Scientific, Bremen, Germany), with a limit of quantification of 0.2 mg/L (Headley et al., 2002; Heshka et al., 2022). Water samples were acidified and eluted under vacuum through a solid phase extraction cartridge (Isolute ENV+, Biotage, Charlottesville, VA, USA). The retained organic fraction was eluted with 6 mL of methanol, evaporated to dryness under nitrogen (5.0 grade, Linde Canada) and redissolved in acetonitrile/Milli-Q water (1:1) with 0.1 % ammonium hydroxide solution. The Orbitrap MS analyses were conducted in full scan negative ion mode, with mass resolution set to 240,000 (as measured at 400 *m/z*) and *m/z* scan range of 100–600. Operation of the ESI source was as follows: sheath gas flow rate 10 (arbitrary units), spray voltage 2.90 kV, auxiliary gas flow rate 5 (arbitrary units), S lens RF level 67 %, heater temperature 50 °C and capillary temperature 275 °C. The mass accuracy was < 2 ppm error for all mass alignments. Analyses were carried out using 5 μL injections introduced via loop injection in 50:50 acetonitrile:water containing 0.1 % NH_4OH at a flow rate of 200 μL/min. Instrument control, data acquisition and pre-processing was done using Xcalibur version 2.1 software (Thermo Fisher Scientific, San Jose, CA, USA) and formula assignment was achieved using Composer version 1.5.2 (Sierra Analyttics, Inc., Modesto, Canada). AEO standards used for MS response calibration were prepared using the method of Rogers et al. (2002) and described by Headley et al. (2011, 2013). Briefly, AEOs in oil sands process-affected water were isolated via liquid–liquid extraction buffered to a pH of 8.0. AEOs in this extract were calibrated against a commercial standard via Fourier Transform Infrared Spectroscopy (FT-IR), whereby concentrations of the standard curve were related to the IR peak absorbance of the extract (Jivraj et al., 1995; Ripmeester & Duford, 2019).

2.3. Embryotoxicity Assays, EROD assays, RNA Extraction, cDNA Synthesis and Real-Time quantitative polymerase chain reaction (RT-qPCR)

Fathead minnow (*Pimephales promelas*) 7-day embryotoxicity assays were conducted in accordance with the US EPA *P. promelas* embryo-larval survival and teratogenicity test method (USEPA, 2002). Fertilized eggs were collected from a minimum of 8 breeding pairs of an established fathead minnow colony at INRS. Eggs were inspected under light microscopy for an absence of abnormalities, and selection of those aged 5.5–7.5 h post-fertilization, of developmental stages 11–13 (Devlin et al., 1996; Marentette et al., 2014). Water from the wave tank (100 % WAF) was serially diluted four times with control wave-tank water to create the range of dilutions used for exposures, 12.15, 25, 50 and 100 % WAF. A total of 12 replicates of 100 mL samples were prepared in 250 mL borosilicate glass beakers with 10 randomly selected embryos placed in each. 7-ethoxyresorufin-O-deethylase (EROD) analyses utilized 5 of the 12 replicates, while RNA extraction was conducted on the remaining 7 replicates. This prevented any sampling bias as EROD and RNA extraction techniques both require whole-body tissue digestion. Daily 85 % static-renewal of exposure media were conducted. Water temperature, pH, conductivity and dissolved oxygen were checked daily. Jars were checked for hatching time and mortality in 24-h intervals, prior to static-renewal, with dead embryos/larvae scored and removed.

Termination of the exposures was followed by a transfer of each individual fish to 100 mg/L of tricaine methanesulfonate (MS-222) buffered 2:1 with sodium bicarbonate (Sigma-Aldrich, St. Louis, MO, USA). Embryos were scored for malformations under light microscopy (Nikon SMZ25 stereomicroscope, Nikon Canada, Mississauga, ON, Canada). Embryos were considered malformed if they exhibited at least one of the following malformations: pericardial or yolk sac edema, tube heart, craniofacial or spinal deformities, reduced or absent swim bladder, and hemorrhages. Larval fish of each replicate were pooled and transferred to a 2 mL centrifuge tube, flash frozen in dry ice, and stored at −80 °C until RNA extraction. All experiment and fish husbandry followed the Canadian Council of Animal Care guidelines and were approved by the INRS Animal Care Committee.

For EROD analyses, *P. promelas* embryos were transferred to 2-ml Eppendorf tubes. A stock solution of 1 mM 7-ethoxyresorufin (7-ER; ≥ 95 %; Millipore Sigma) was prepared in DMSO following the protocol used by Gutierrez-Villagomez et al. (2024). From the 7-ER stock solution, a 1 μM 7-ER solution was prepared with reconstituted water and 1200 μL of 7-ER 1 μM was added to each tube. A standard curve for fluorescence with resorufin (95 %; Millipore Sigma) was prepared in reconstituted water (0–10 nM). After 4 h of incubation at 25 ± 1 °C, 100-μL aliquots were transferred from each tube to a dark Thermo Scientific Microwell 96-well microplate. The standard curve was run with three technical replicates, while the samples were run in technical duplicates. The fluorescence was determined using a FilterMax F5 Multi-Mode Microplate Reader (Molecular Devices, San Jose, Califronia, USA) at an excitation wavelength at 544 nm and emission at 590 nm. At the end of the assay, the embryos were sacrificed and stored at −80 °C. The amount of protein was assessed using the Coomassie (Bradford) protein assay kit (Thermo Scientific, Waltham, MA, USA) following the manufacturer's protocol. Briefly, 500 mL of phosphate-buffered saline (PBS) was added to the samples prior to homogenization using a stainless-steel ball (5 mm) and a Retsch® mixer mill MM 400 (FisherScientific®, Waltham, MA, USA) for 2 min at 20 Hz. An absorbance standard curve at

595 nm for albumin concentrations from 0-2000 μg/mL was included in each plate (Thermo Scientific, Waltham, MA, USA). Five μL of the albumin standard and the samples were transferred to a transparent 96-well microplate and 250 μL of the Coomassie dye was then added to each well. The plate was left in the dark for 10 min and the absorbance was measured at 595 nm in a VARIOSKAN LUX spectrophotometer (Thermo Scientific, Waltham, MA, USA). The standard curve was run with three technical replicates, while the samples were run in technical duplicates. The EROD activity was expressed as picomole of resorufin per microgram of protein per microgram of sample.

Total RNA was isolated from the fish larvae using the RNeasy Micro Kit (Qiagen, Hilden, Germany) as described in the manufacturer's protocol. Total complementary DNA (cDNA) was prepared using Maxima™ H Minus cDNA Synthesis Master Mix with dsDNase (Thermo Fisher Scientific) as described in the manufacturer's protocol. The qPCR analyses were performed on CFX96 thermocycler (Bio-rad, Hercules, California, USA) with Maxima SYBR green (Thermo Scientific, Waltham, MA, USA) following the manufacturers protocol (Bérubé et al., 2023; Gutierrez-Villagomez et al., 2019a).

The cytochrome P450 1A gene (*cyp1a*) involved in petroleum detoxification was studied. Total RNA was isolated from the fish larvae using the RNeasy Micro Kit (Qiagen, Hilden, Germany) following the manufacturer's protocol. RNA integrity and the concentration of all samples were measured using a NanoDrop ND-2000 spectrophotometer (Thermo Fisher Scientific, Waltham, MA, USA) and a 1 % agarose gel. The RNA integrity was also assessed on an agarose gel by the presence of two bands representing the 28S ribosomal RNA subunit (rRNA) and 18S rRNA (Aranda et al., 2012). Samples failing the integrity test were removed from the set of samples. Total complementary DNA (cDNA) was prepared using Maxima™ H Minus cDNA Synthesis Master Mix with dsDNase (Thermo Fisher Scientific, Waltham, MA, USA) in a Mastercycler® nexus gradient (Eppendorf, Hamburg, Germany) as following the manufacturer's protocol and stored at −20 °C. During cDNA synthesis, no reverse transcriptase (NRT) and no template controls (NTC) were included.

For *myod* qPCR primers, they were designed on conserved region sequences of other fish species obtained by degenerate primers sequencing developed in this study (Table S1). Gene-specific primers based on sequences of *Pimephales promelas* were designed with Primer-Blast (NCBI) and synthesized by Sigma Aldrich (Table S2). The primers for *cyp1a* were previously reported (Alsaadi et al., 2018; Jacobo et al., 2021), and other primers were designed and optimized by our team (Table S2). To confirm the amplification of the regions of interest, the PCR products were analyzed on 2 % agarose gel and then purified using the NucleoSpin® Gel and PCR Clean-Up kit (Takara), sent to the Centre Hospitalier de l'Université Laval and sequenced using 3730 DNA Analyzer (Applied Biosystems, Waltham, MA, USA).

The Maxima SYBR Green qPCR Master Mix (Thermo Fisher Scientific) and CFX96 Real-time PCR Detection System (Bio-Rad) were used for amplifying and detecting transcripts of interest. The qPCR thermal cycling parameters followed manufacturer suggestions with an activation step at 95 °C for 10 min, followed by 40 cycles of 95 °C denaturation step for 15 s and one primer annealing/extension temperature depending on the primer set for 60 s (Table S2). After 40 cycles, a melt curve was performed over a range of 60–95 °C with increments of 0.5 °C to ensure a single amplified product. The final concentration of each primer in all of the RT-qPCR reactions was 0.3 μM. The final volume in all of the reactions was 20 μL. Progene® thin-wall PCR strip tubes and PCR 8-Strip flat optically clear caps for qPCR were used for the reactions.

The efficiency of all RT-qPCR reactions was 98.8 ± 6.1 % and the coefficient of determination (R^2) was ≥ 0.990 (0.994 ± 0.002). Data were analyzed using the Bio-Rad CFX Manager Software. The relative standard curve method was used to calculate relative mRNA abundance between samples (Gutierrez-Villagomez et al., 2019b; Lebordais et al., 2021). The signal was normalized using the reference genes *ef1α*, *myod,* and *rpl8* and then presented as fold change of gene expression from replicates (n = 11–16; assayed in duplicate) for each group.

2.4. Data processing and statistical analysis

Analysis of outliers was performed using the ROUT method (Q=1%) in GraphPad Prism 8 (Motulsky & Brown, 2006). To assess data normality and homogeneity of variance, Shapiro–Wilk's test and Levene's test were performed, respectively. Data that failed the normality and/or the equal variance tests were transformed (squared root-squared root and Log_{10}). One-way ANOVA and post hoc Student–Newman–Keuls (SNK) analyses were performed on normally distributed data. Non-parametric Kruskal–Wallis tests were performed on data that did not pass normality and/or equal variances tests followed by Dunn's method for unequal sample sizes. The significance level was set at $\alpha = 0.05$. One-way ANOVA analyses were performed using Sigma Plot 12.0 (company, city, state, country. The significance level was set at $\alpha = 0.05$. The RcolorBrewer pallet was used to assign colorblind-friendly colours to the graphs (Neuwirth, 2014).

3. Results

3.1. Mortality

Mortality for fish exposed to water contaminated with either DB or CC was greatest at Day 1 after the oil was spilled with levels of 92.3 ± 10.9 % and 98.7 ± 3.4 %, respectively (Fig. 1). Interestingly, higher mortality was found for water contaminated with DB than for CC for up to 14 days post spill. The DB-contaminated water had mortality between 59 – 82 % while CC-contaminated water mortality levels decreased to those of the control tests after Day 1. Mortality was also observed for fish exposed to the dilutions of the CC water Day 1 post spill (42 – 83 %); mortality for dilutions of DB Day 1 water decreased to control levels (Fig. S2A).

3.2. Sublethal toxicity

3.2.1. Malformations

Developmental malformations included yolk sac and pericardial edemas as well as spinal, craniofacial, tube heart and swim bladder abnormalities (Figure S3). Exposure to undiluted and 50 % WAF of either DB- or CC-contaminated water induced developmental malformations in 100 % of the fish exposed during their embryologic development throughout the 56 days of weathering (Figure S2, S4 and S5). The prevalence of malformations was less severe in the 25 and 12.5 % WAF dilutions, where significantly more malformations were observed in the fish exposed to CC. This was most evident in the 12.5 % dilution, where fish exposed to DB were not significantly greater than the controls (4–13 %) while those exposed to CC had 96, 52, 72 and 77 % of fish malformed on Days 1, 7, 21 and 28, respectively. No differences were observed in the type of malformations caused by either the DB or CC exposures. Decreasing prevalence of malformations with time was observed in the 25 % dilutions of the DB and CC contaminated waters, as there were significantly reduced levels of pericardial edema, spinal, craniofacial, tube heart and swim bladder by the end of the 56 days of weathering. Within the 12.5 % WAF dilutions, the prevalence of malformations of CC exposed fish were significantly greater than the controls and DB on Days 1, 21 and 28.

3.2.2. Heart rate

Larval fathead minnows exposed to both DB and CC undiluted contaminated water during the 56 days of experimentation had heart rates that averaged 126 ± 5 and 84 ± 2 beats per minute (BPM), respectively (Fig. S2C). These rates were significantly lower than the control fish at 193 ± 4 BPM. The notably lower averaged heart rates in CC-exposed fish were about 33 % less than those of fish exposed to DB; however, no significant differences in heartrate were observed between

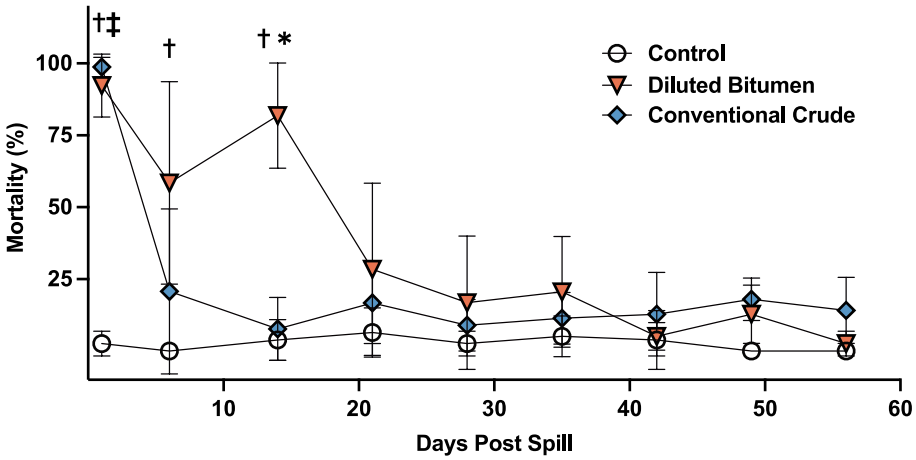

Fig. 1. Proportion of fish mortalities (%) observed following 7-day fathead minnow (*Pimephales promelas*) embryotoxicity assays from spill-tank water collected at designated days post spill of either Cold Lake Blend diluted bitumen (red triangles) and Mixed Sweet Blend conventional crude oil (blue diamonds), or non-oiled control water (white circles). Symbols denote significantly different values between control fish and fish exposed to dilbit (†) or conventional crude oil (‡), or between the two oil types (*) as indicated by two-way ANOVA and post-hoc Tukey analyses ($p < 0.05$). (For interpretation of the references to colour in this figure legend, the reader is referred to the web version of this article.)

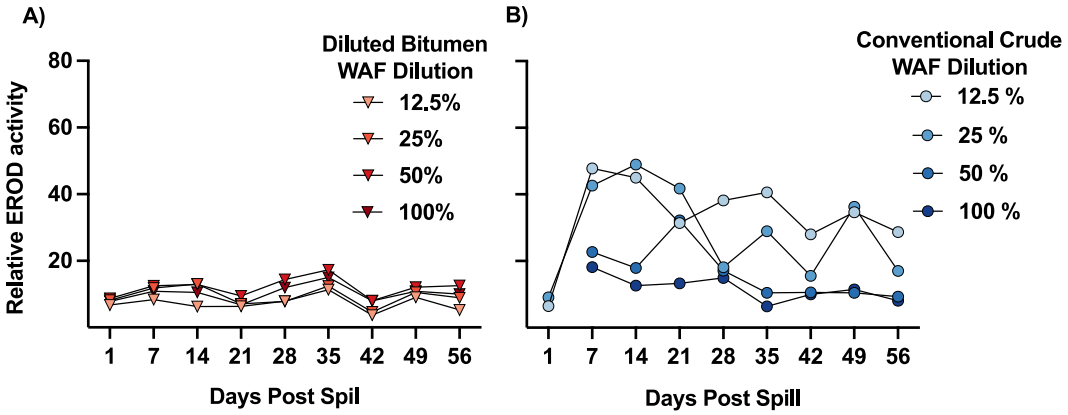

Fig. 2. Relative ethoxyresorufin-O-deethylase (EROD) activity measured *in vivo* for fathead minnow (*Pimephales promelas*) larvae exposed to the water accommodated fraction (WAF) dilutions following the spill of (**A**) Cold Lake Blend diluted bitumen or (**B**) Mixed Sweet Blend conventional crude oil. EROD activity was measured in units of picomole of resorufin per milligram of protein and was normalized to the value of the respective negative control. Error bars representative of standard deviation from the mean.

the two oil types on Days 6 and 35. Similar trends were observed in the dilutions, with a negative correlation between the degree of dilution and the severity of heart rate reduction. For the 12.5 % dilutions, the heart rates for fish exposed to DB water were not different than the controls, and for CC were significantly lower than the control and DB on Days 1, 21 and 28, similar to the prevalence of malformations.

3.2.3. Body length

Exposure to either DB or CC during embryologic development resulted in larval fish with body lengths approximately 14 or 21 % less than those of the controls (Fig. S2D). Throughout the 56-days of experimentation, the fork length of fish exposed to DB or CC averaged around 4.6 ± 0.0 and 4.1 ± 0.0 mm, whereas control fish were 5.3 ± 0.1 mm. Reductions in body length were greatest when exposed to water contaminated with either DB or CC 1 day after the oils were spilled, with the fish averaging body lengths of 28 and 32 % less than those of the controls (3.8 and 3.6 mm, respectively). Similar to heart rate, the severity of reductions in body length were negatively correlated with the degree of dilution. No significant differences were observed between the fork length of control larval fish and those exposed to the 12.5 and 25 % dilutions of DB-contaminated water. However, body lengths of CC-exposed fish were significantly less than the control fish at about 90 % the length (4.9 mm) after exposure to the 25 % dilution (except for Days 42 and 49) and were significantly less than the DB-exposed fish on Days 1, 21, 28 and 35. For the 12.5 % dilution, CC-exposed fish were about 12 % shorter in body length (0.4 mm) than the controls on Days 21, 35 and 56.

3.3. Biomolecular response

3.3.1. CYP1A activity

Figs. 2 and S2E show the results of relative EROD activity for the fish exposed to oil contaminated water. Water contaminated with DB induced relatively low levels of EROD activity in the range of 5 to 18 times greater activity than the control over the 56 days, at all dilutions. There were slight reductions of effects with dilution. For CC-contaminated water, the 100 % WAF had the lowest relative EROD activity starting at 19-times greater activity than the control at Day 7 and trending down to 10-times greater activity at Day 56. For CC WAF dilution samples, EROD activity gave widely variable results from 6- to 50-times the activity of the controls with no apparent correlation with time.

3.3.2. CYP1A gene expression

Expression of *cyp1a* mRNA in DB exposed fish was significantly greater than for fish exposed to CC throughout the 56 days and at each dilution, with the exception of Day 1 (Fig. S2F). CC-exposed fish on Day 1 had significantly greater levels of *cpy1a* than those of DB within the 50 and 12.5 % dilutions. No apparent relationships were observed between dilutions or with time, with the CC-exposed fish *cyp1a* levels between 1- to 13-fold greater than the controls, and the DB-exposed fish between 9.5- to 138-fold greater than the controls.

3.4. Crude oil weathering

3.4.1. Crude oil compositions and properties

As discussed in our companion microbial study (Xin et al., 2024), DB had higher density, was more viscous and had greater interfacial tension than CC (0.9264 versus 0.8216 g mL^{-1}, 268 versus 4 cSt at 25° C, and 16.6 versus 12.2 mN m^{-1} at 20 °C, respectively). High temperature simulated distillations (HTSD) demonstrated the composition of DB to be 83 wt% organic compounds with a boiling point above 204 °C (10 carbons and larger in size; C_{10} +) and 17 wt% volatile compounds boiling point below 204 °C, versus 67 wt% C10 + and 33 % volatiles for CC. The higher composition of C_{10} + compounds in the DB correlated with final floating oil at the end of the 56 days having lost only 21 % of organic compounds with boiling points less than 233 °C, whereas CC lost 49.1 % of organic compounds with a boiling point less than 271 °C (Figure S6).

3.4.2. Water chemistry profile

Water pH, electrical conductivity and temperature did not change significantly following the addition of oils to the freshwater, or over the 56 days of weathering (Table S3). TOC increased rapidly from the background river water levels of 2.6 mg L^{-1} to 22.0 mg L^{-1} within the first hour following the spill of CC yet rose to only 8.6 mg L^{-1} after 6 h following the spill of DB (Figure S7). TOC concentrations then decreased to approximately 4.0 mg L^{-1} between Days 1 to 7 for both DB and CC, with concentrations rising steadily to about 8.0 mg L^{-1} by Day 56. Trace elemental analyses demonstrated no significant changes in the concentrations of metals following the spills of both oil types (Table S4 and S5).

3.4.3. Aromatic compounds

Concentrations of monoaromatic compounds measured in spill-tank water included benzene and select alkylated homologs (Table S6). Concentrations of total MACs were greatest following 1-day, with DB-exposed water containing 460 µg L^{-1} and CC-exposed water approximately 2-fold greater at 801 µg L^{-1} (Fig. 3). This ratio matched the original MAC composition in each crude oil, with DB containing 1 % BTEX by weight and CC containing 2.2 %. MACs in DB were mainly composed of toluene, benzene and xylenes (170, 146 and 120 µg L^{-1}, respectively) and xylenes and trimethylbenzenes (590 and 150 µg L^{-1}, respectively) in CC. Concentrations decreased to 8.98 and 2.43 µg L^{-1} in DB and CC, respectively, by Day 7 and were below 1 µg L^{-1} from Days 14 to 56 for both oils, except for Day 21 whereby concentrations reached 1.71 µg L^{-1} in the water amended with CC. Similar trends were observed in the serial dilutions of both DB and CC water (Figure S8).

Concentrations of PACs 1 day post oil spill were significantly greater in the CC-contaminated water (13,677 µg L^{-1}) than the DB-contaminated water (94 µg L^{-1}; Fig. 3). This 145-fold greater concentration in CC rapidly dissipated to 296 µg L^{-1} on Day 7, followed by fluctuations between 45.0 – 358 µg L^{-1} until Day 56. PAC concentrations in the DB spill-tank increased gradually after the spill to 561 µg L^{-1} on Day 21, followed by a rapid decrease to 70 µg L^{-1} and subsequent plateau from Day 28 to 56. The composition of PACs measured within the water of the CC and DB spills throughout the experiment were dominated by 2–3 ring parent PACs and their alkylated homologs (C_1-C_4), with naphthalenes being most abundant (approximately 50 % of the PACs measured for both oil types), followed by phenanthrenes (19 % for CC and 15 % for DB), fluorenes (12 and 9 %, respectively) and dibenzothiophenes (5 and 13 %, respectively). Dissipation over time was most evident for the 2- and 3-ring parent PACs (*i.e.*, naphthalene, fluorene, dibenzothiophene, phenanthrene, fluoranthene), with their respective alkylated homologs persisting for a longer duration throughout the 56 days of weathering.

3.4.4. Total petroleum hydrocarbons

Concentrations of TPHs of C_{10}-C_{50} (including the aliphatics) compounds within the water containing spilled CC were highest on Day 1 for CC at 520 mg L^{-1}, which decreased rapidly to 31 mg L^{-1} on Day 7 and fluctuated between 8.9 and 85 mg L^{-1} until Day 56. Concentrations of C_{10}-C_{50} in the water amended with DB fluctuated from 2.2 and 6.0 mg L^{-}

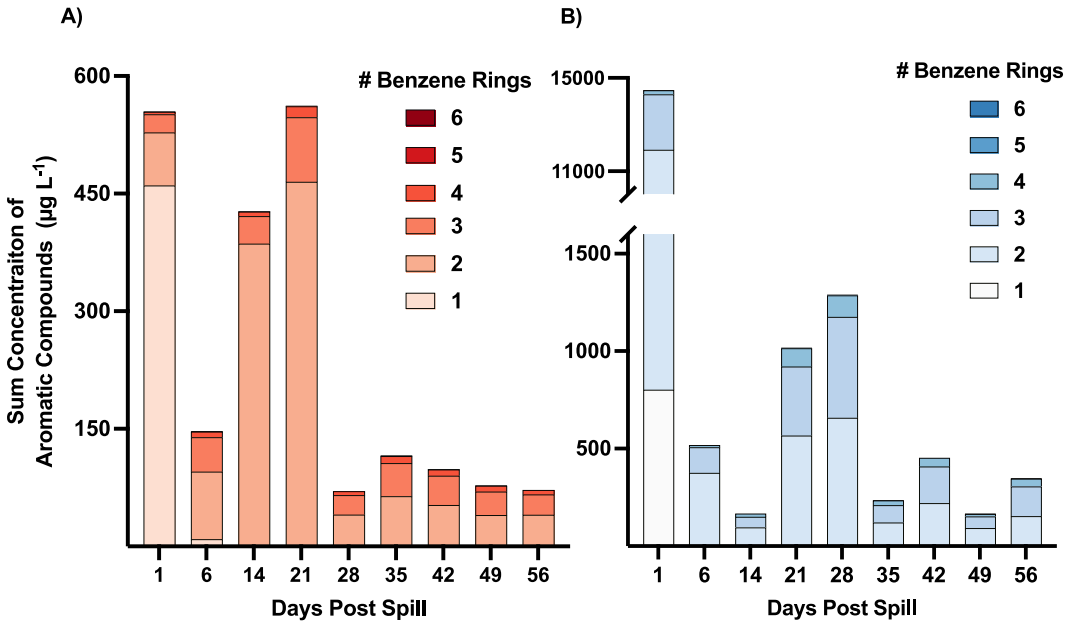

Fig. 3. Sum concentration (µg/L) of both parent and alkylated aromatic compounds by the number of benzene rings, measured within water with **(A)** spilled Cold Lake Blend diluted bitumen or (**B**) Mixed Sweet Blend conventional crude oil.

^{1} between Days 1 to 56. Similar trends were observed in the serial dilutions of both DB and CC water (Figure S8).

3.4.5. Oxygenated acid extractable organics (AEOs)

Rapid increases were observed in the levels of oxygen-containing AEOs within the water of both oil spills; however, these relative abundance levels plateaued by Day 2 and subsequently remained constant for DB, while a rapid dissipation and gradual increase from Day 1 to Day 18 was observed in the CC-exposed water (Fig. 4). The relative abundance of the most prevalent oxygen-containing species classes detected in the AEO fraction are shown in Fig. 5. Within the first hour post-spill, organic acids within the water of spilled DB and CC were dominated by species containing a single oxygen (50 and 36 % relative abundance, respectively). These levels considerably decreased by Day 2 (1 and 11 %, respectively) whereby O_2 species rose to 90 and 38 % for DB and CC, respectively. These O_2 abundances decreased gradually throughout the remainder of the weathering experiment, whereby respective increases were observed for O_3 and O_4 in the water for both oil types, and in O_3S species specifically for CC.

4. Discussion

4.1. Acute toxicity

Early life stage fathead minnows exposed to DB-contaminated water at 24 °C exhibited acute lethality (>58 % of exposed fish) for up to 14 days post oil spill, whereas CC-induced lethality for water prepared similarly occurred only within the day of the spill. Significantly increased acute toxicity for a 14-fold greater duration of time provides strong evidence that variability exists between DB and CC to cause significantly distinct risks to aquatic organisms following freshwater spill events.

Within the last half-century, numerous studies have attempted to characterize the petroleum constituents responsible for crude oil toxicity following accidental spill events (Hodson, 2017; Incardona, 2017; Meador & Nahrgang, 2019). Focus has largely been on the aqueous concentrations of petroleum-derived organic compounds in the WAF based on its potential bioavailability and intrinsic toxicity (Carls et al., 2008). Most studies to date have concluded that MACs and PACs are the petroleum constituents principally responsible for the acute and sublethal toxicity of crude oils, with aromatic compounds consisting of two benzene rings or less (LMW aromatics) specifically inducing acute lethality (Bérubé et al., 2021; NASEM, 2022; Philibert et al., 2016). The general consensus that these LMW aromatics are more lethal to aquatic organisms has been attributed to their relatively greater bioavailability compared to the higher molecular weight PACs (3 rings or more). This can be attributed to the greater water solubility of LMW aromatics and their more rapid rate of uptake into organisms as compared to larger PACs (Lee et al., 2015; McGrath & Di Toro, 2009).

Within our own study, concentrations of MACs and PACs in the water of both the DB and CC spills were their highest 1 day post oil spill, which coincided with the highest mortality (92 and 98 % for DB and CC, respectively). MAC concentrations were nearly 2-fold greater in the water of spilled CC (801 μg L^{-1}) compared to DB (460 μg L^{-1}), surpassing water quality guidelines for the protection of aquatic life set out by the Canadian Council of Ministers of the Environment or Canadian provincial regulating bodies (370, 90, 2, and 32 μg L^{-1} for benzene, toluene, ethylene and xylene, respectively; (BCME., 2007; CCME, 1999a, 1999b, 1999c). Within the water of both oil spills on Day 1 of our study, naphthalene and its alkylated homologs dominated the composition of PACs within the water of DB and CC (greater than 40 and 60 % of total PACs, respectively). Several studies have demonstrated that the 96 h LC_{50} (concentration that will induce lethality to half of exposed organisms during a 96-h exposure) for fathead minnow adults exposed to naphthalene alone is in the range of 6,080 – 7,900 μg L^{-1}. Naphthalene concentrations measured in the CC water on Day 1 of our study were 8,370 μg L^{-1}, thus along with concomitant exposure to the suite of other measured petroleum compounds during our 7-day embryo life-stage exposures, lethality was expected.

Notably, however, lethality was not observed for fish exposed to serial dilutions of DB water (12.5, 25 and 50 % WAFs) whilst lethality was significantly elevated for fish exposed to CC dilutions. Such acute toxicity in the CC dilutions could be rationalized by the significantly higher concentrations of aromatics, which were more than 67-fold greater than those measured in DB water (Table S7). However, the concentrations of aromatics did not explain the significantly elevated mortality for fish exposed to DB water up to Day 14, as MACs were negligible beyond Day 1 and PACs were up to 3-fold less than those measured in CC water. Furthermore, the concentrations of total petroleum hydrocarbons (C_{10}-C_{50}) measured were lower in the DB-contaminated water between Days 1 – 14 (2.2 – 3.9 mg L^{-1}) than any of the time points for CC (10 – 520 mg L^{-1}).

Indeed, the water-soluble fraction of crude oils is not only limited to those quantifiable with gas chromatography techniques (e.g., aliphatics, aromatics). The UCM of crude oils can contain upwards of 250,000 unidentified compounds and can comprise up to around 70 % of the water-soluble fraction (Cho et al., 2012; Sutton et al., 2005). Separating crude oils into 14 different fractions of increasing polarity, Melbye and colleagues (2009) were able to demonstrate that the greatest in-vitro toxicity to rainbow trout liver cells was not caused by fractions dominated by aromatics, but those dominated by unidentified polar compounds. A recent groundwater transport study by Hepditch et al. (2024) demonstrated that the elution of such polar compounds within the acid extractable organics (AEOs) fraction occurred while aromatic content was at its lowest, yet the discharged groundwater caused significant toxic effects for fathead minnow embryos.

Using the same analytical technique (Orbitrap MS), in the present study we observed rapid increases in AEO concentrations following the

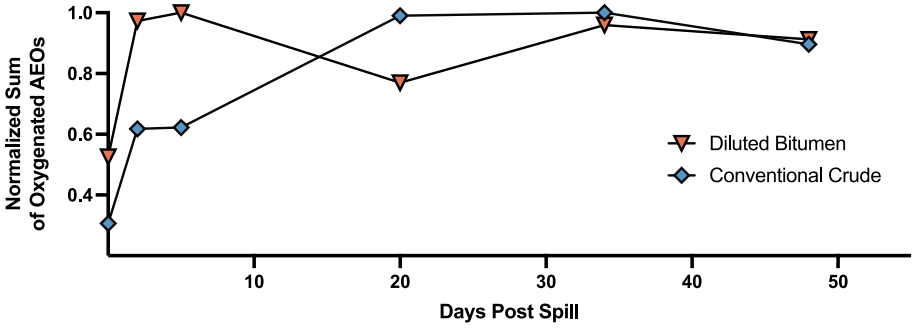

Fig. 4. Sums of semi-quantitative orbitrap MS analysis of oxygen-containing species within the acid extractable organics (AEOs) fraction of water samples following spills of Cold Lake Blend diluted bitumen or Mixed Sweet Blend conventional crude oil. The concentrations measured at each time point were divided by the highest observed concentration for that respective oil type, providing comparison between these semi-quantitative analyses.

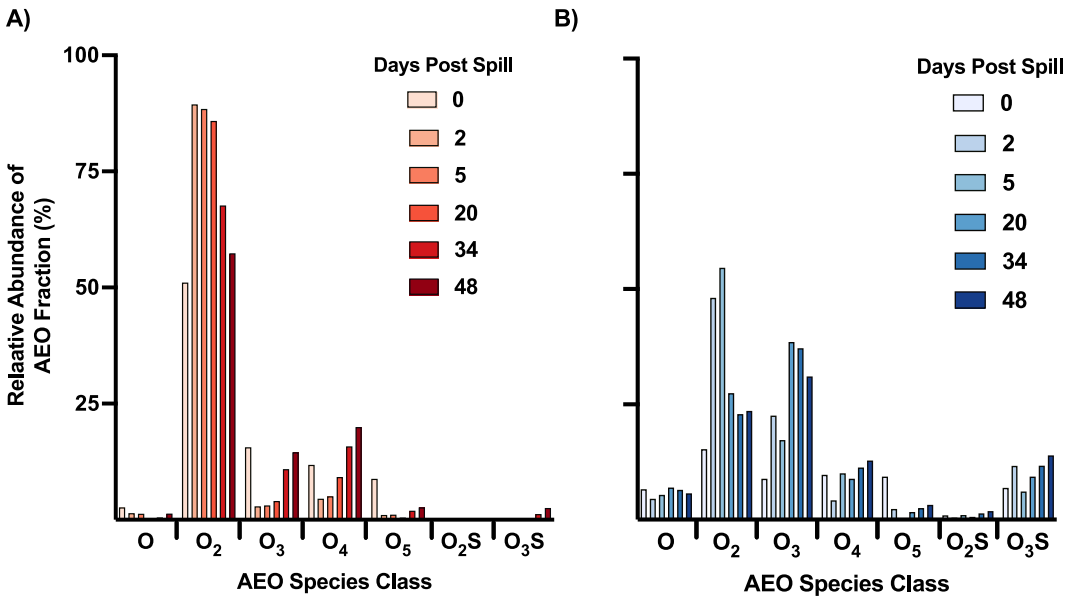

Fig. 5. Relative abundances of oxidized species classes detected within the acid extractable organics (AEOs) fraction of water samples following spills of (**A**) Cold Lake Blend diluted bitumen or (**B**) Mixed Sweet Blend conventional crude oil.

spills of both oil types (Fig. 4). However, the initial increase in CC-contaminated waters was more transient as AEOs decreased sharply by Day 5, whereas DB-exposed water reached its peak abundance that remained relatively consistent until the end of the 56-days of weathering. The AEOs of DB-exposed water were dominated by organic acid O_2-containing species (90 %), which decreased sharply following Day 20 with the concomitant increase of O_3 and O_4 species over time. Similar results were observed in the companion analytical study of our experiment by Monaghan et al. (2022), whereby condensed phase membrane induction mass spectrometry (CP-MIMS) analyses demonstrated an increase in the abundance of the organic acids (*i.e.*, O_2-containing species) up until Day 14, followed by their rapid decay and subsequent dissipation. Organic acids found in crude oils and their process waters often result from the partial biodegradation of the organic compounds in the oils either in the reservoir, or in contaminated surface water. Included in this fraction are the classically defined naphthenic acids, alkyl-substituted, acyclic and cycloaliphatic carboxylic acids that have the general formula $C_nH_{2n+Z}O_2$, where C is the number of carbon atoms (usually 10 to 20 detected by techniques used herein) and Z is the hydrogen deficiency due to the presence of rings and/or double bonds (usually −2 to −10; Speight, 2019). Isomer class profile identification of this AEO fraction of DB water within the first 14-days by Monaghan et al. (2022) using full scan mass spectra analyses coupled with orbitrap MS demonstrated peaks primarily associated with the classical "O_2" naphthenic acid species of $C_{15}H_{26}O_2$ and $C_{16}H_{28}O_2$. Notably, recent use of orbitrap MS by Hughes et al. (2017) had demonstrated that these C_{15}-C_{16} classic naphthenic acids were of those responsible for the acute toxicity of oil sands process affected waters (OSPW) resulting from oil biodegradation during water-intensive extraction and processing of bitumen oils in Western Canada. Due to the semi-quantitative methods used for analyzing these naphthenic acids, direct comparisons of absolute concentrations would not be recommended. However, this method provides a high resolution of molecular compound characterization and relative quantitation. Within our companion study by Monaghan et al. (2022), characterized classic naphthenic acids were determined to have half-lives of approximately 39–48 days. Furthermore, an additional study by Monaghan et al. (2021) demonstrated that water contaminated with a spill of DB contained 10-fold greater concentrations of naphthenic acids than water amended with CC. Therefore, it is reasonable to assume that the 14-day-longer period of lethality to fathead minnow larvae within the DB water as compared to CC was likely a function of the greater prevalence of the classic naphthenic acids present.

Throughout the duration of the 56 days of weathering the relative abundance of O_2 compounds decreased within the water of both DB and CC, whereby concomitant increases in the more oxidized O_3, O_4 and O_3S species were observed (Fig. 5). Evidence of oxidation reactions was shown when comparing the decreasing abundance of O_2 species which consisted of compounds with 13–16 carbon atoms and 2–4 double bond equivalents (DBEs) that were present immediately following the oil spill versus the increasing abundance of compounds with 11–14 carbon atoms and 5–7 DBEs (Monaghan et al., 2022). Although photodegradation was unlikely due the low-intensity LED lights (producing minimal ultraviolet radiation) within our experiment, microbial degradation of petroleum compounds was demonstrated in a companion study to our experiment by Xin et al. (2024). Microbial community compositions and diversity showed strong correlations to the most abundant petroleum constituents in the water column (*i.e.*, aromatics and AEOs), with a dominant proliferation of Actinobacteria only within the water of DB spill between Days 5 to 28. Actinobacteria have been demonstrated to be highly effective at degrading classic naphthenic acids (Johnson, 2011; Zhang et al., 2018) and are prolific in environments with high concentrations of these compounds, such as soils recently contaminated with CC oil or DB spills (Mindorff et al., 2023) or in waters contaminated with OSPW in Western Canada (Ahad et al., 2018; An et al., 2013). The proliferation of Actinobacteria measured in DB-exposed water correlates well with the degradation rates of the classic naphthenic acids measured by Monaghan et al. (2022) and demonstrates their role in the natural weathering of dilbit constituents throughout the 56 days of weathering.

4.2. Sublethal toxicity

Throughout the 56 days of DB and CC oil weathering within our spill tank study, acute lethality for exposed fathead minnows was negligible beyond 14 days; however, sublethal toxicity measured through the presence of developmental malformations, reduced heart rates and body lengths remained significantly elevated. Additionally, these toxic effects were significantly more pronounced in fish exposed to CC– compared to DB-contaminated water throughout the 56 days of weathering. Greater bioavailability of aromatics and TPHs was evident by their higher

concentrations in CC-exposed water, correlating with a higher observance of sublethal effects. PACs and their alkylated homologs are often identified as the petroleum constituents that contribute most to the sublethal embryotoxicity of crude oils, evidenced by numerous studies correlating their exposure to developmental abnormalities (Cherr et al., 2017; Hodson, 2017; Lee et al., 2015). PAC exposures during embryologic organogenesis is well correlated to a very characteristic toxicity syndrome with symptoms that include cardiac deficiencies, fluid accumulation around the heart and yolk-sac (edemas), and craniofacial and spinal abnormalities (Incardona, 2017). Within the context of the current study, the increasing severity of this petroleum toxicity syndrome correlated strongly with the increasing bioavailability of PACs. This was confirmed by the dilution-response effect observed, with the 100 % WAF being the most toxic, and by the greater severity of the sublethal malformations observed for the fish exposed to the higher PAC content of the CC– versus DB-contaminated water.

Greater sublethal toxicity for malformations, reduced heart rate and length was observed on Day 1 for both DB and CC experiments, when the highest sum of aromatics were measured in the water for both oil spills. The rapid dissipation of aromatics from Day 1 to 14 in the water of the CC spill correlated with reductions in these sublethal effects during this time. The ensuing increase in PAC concentrations on Days 21 and 28 and decrease in concentrations on Day 35 were matched by similar fluctuations in the degree of sublethal toxicity, which was most evident in the fish exposed to WAF dilutions of CC-amended water. The sublethal toxicity of DB WAF was not as well correlated; however, with the highest concentrations of PACs on Day 21 (PACs at 561 μg L^{-1}), yet the impacts upon heart rate and fork length were either similar or not as toxic as the time points with the lowest measured aromatic content (Days 28–56).

Although PACs have been promulgated to be principally responsible for the sublethal toxicity induced by crude oils, up to 25 % of the variation in the sublethal toxicity induced by petroleum PAC congeners is unexplained (Hodson, 2017). Adverse outcome pathways induced by 3- and 4-ring PAC compounds have been linked to the downregulation of genes encoding components that regulate the K^+ and Ca^{2+} ion cycling necessary for cardiomyocyte excitation and contraction coupling (Brette et al., 2017; Incardona, 2017). Interestingly, benzenes and naphthalenes are assumed to not contribute to such sublethal toxicity (Incardona et al., 2004), yet fish heart rates and lengths in our study were most severely impacted by DB-exposed water at peak concentrations of these volatile compounds on Day 1, when 3- and 4-ring PAC concentrations were lowest. The lack of consistency between the observed sublethal effects on development and growth to the fluctuations in PAC concentrations for the fish exposed to spilled DB may therefore suggest the bioavailability of other petroleum toxicants.

Indeed, the high concentration and subsequent dissipation of oxidized compounds in DB-exposed water with time correlates well with the observed acute lethality for fish exposed to DB water and would therefore likely contribute to the sublethal toxicity observed within the first 14 days of the experiment. The sublethal toxicity of naphthenic acids to embryologically developing fish has been well characterized from studies on OSPW, with symptoms indistinguishable to those of the toxicity syndrome induced by crude oils and PACs (Li et al., 2017; Marentette et al., 2015). This syndrome is also well correlated to sublethal effects from the non-specific mechanism of baseline toxicity, also referred to as narcosis, which has been identified for numerous organic contaminants, including PACs (Escher et al., 2011; Meador & Nahrgang, 2019). Baseline toxicity itself is an impairment of cellular lipid membrane integrity and function as a consequence of the influx and deposition of, typically, organic toxicants. This mechanism of toxicity has been demonstrated for both naphthenic acids (Frank et al., 2009a; Roex et al., 2000) and PACs (Di Toro et al., 2000; McGrath & Di Toro, 2009), and is one of the most reliable predictors of both acute and chronic toxicity when modeling the risks of spilled crude oils and fuels (French-McCay et al., 2023). Acute and sublethal effects occur at relatively precise critical membrane concentrations (lethal body burdens) of individual baseline toxicants and can be predicted by their dissociation between lipid and aqueous phases, commonly characterised by the octanol–water partitioning coefficients ($\log_{10} K_{ow}$; Mcgrath et al., 2018; Scholz et al., 2018). Toxicokinetic transport of baseline toxicants capable of permeating cellular lipids ($\log_{10} K_{ow}$ = 3–6) is heavily influenced by polarity, whereby steric factors influence physicochemical interactions within living cells. Less polar toxicants can permeate within untargeted lipids, whereby intercalation of the more polar toxicants would be restricted to the polar head groups of lipid membranes (Escher et al., 2011). Lethal body burdens of polar baseline toxicants are consequently lower than those less polar, and thus considered more toxic. This would explain why greater aquatic toxicity was observed by Frank et al. (2009a) for naphthenic acids of linear structural conformation compared to more clustered structural arrangements. Furthermore, the toxicity of naphthenic acids has been shown to decrease with increasing number of carboxylic groupings, which would both reduce polarity and increase $\log_{10} K_{ow}$ (Frank et al., 2008; Frank et al., 2009b). The oxidation of the O_2 naphthenic acids present in our experiments ostensibly via microbial degradation would have therefore reduced both their lethal and sublethal toxicity, explaining the greater lethality and impaired development observed for fathead minnows within the first 14 days post oil spill.

Although oxidation of certain naphthenic acids may reduce their toxicity, the oxidized products may have potentially contributed to the observed sublethal toxicity (Marentette et al., 2015). This is evidenced by the comparatively similar or greater sublethal toxicity of 25 % WAF of the DB-contaminated water as compared to the 12 % WAF of the CC-contaminated water, as depicted by the proportion of malformations observed in Figure S9. Within this comparison, toxic units were predicted based on the Quantitative Structure-Activity Relationships presented by Mcgrath et al. (2018), which normalize the summed concentrations of PACs based on each PAC's predicted probability to induce baseline toxicity (French-McCay et al., 2023). Following Day 35 of our weathering experiments, it is evident that greater malformations were induced by the 25 % WAF of DB water despite it having a substantially lower predicted toxic effect than the 12.5 % WAF of CC when only accounting for the toxicity of PACs. As the classical and oxidized naphthenic acids are known to be baseline toxicants that can induce similar sublethal effects as those caused by PACs, their greater concentrations in the DB water would explain the relatively greater sublethal toxicity despite having significantly lower PAC concentrations than the CC spill.

Much attention has been directed to the potential risks imposed by the oxidation of petroleum hydrocarbons following accidental spill events in recent years. Similar to naphthenic acids, the presence of oxidized hydrocarbons from either terrestrial or aquatic petroleum spills have been correlated to acute and sublethal toxic effects characteristic of baseline toxicity syndrome (Bekins et al., 2020; Podgorski & Bekins, 2023). The oxidation of petroleum compounds in crude oils can subsequently increase the water solubility and thus bioavailability to receptive aquatic organisms. Furthermore, the toxicity of oxygenated petroleum compounds has been demonstrated to be comparable to or greater than PAC compounds (Fallahtafti et al., 2012; Mccarrick et al., 2019; Schrlau et al., 2017). Recent work by Donald et al. (2023) has demonstrated that the oxidation of bioaccumulated phenanthrene via cytochrome P450 (cyp1a) Phase I metabolism within early life stage fish significantly increased the prevalence of developmental toxicity.

Within our own study, such Phase I oxidation of bioaccumulated petroleum compounds was likely for both DB and CC, as evidenced by significantly elevated CYP1A biotransformation activity (measured via EROD activity) and *cyp1a* gene expression. Notably, however, EROD activity was relatively similar for fish exposed to all WAF dilutions of DB water, yet activity was reduced when PAC concentrations were elevated in CC water. Enzymatic inhibition and extensive cellular damage have both been correlated to reduced CYP1A activity following high concentration crude oil exposures in fish (Kais et al., 2018; Pathiratne &

Hemachandra, 2010; Shailaja & D'Silva, 2003). This would serve as a plausible explanation for reduced CYP1A activity observed with increasing PAC concentrations for the CC exposures. Although generally less potent than PACs, some oxidized petroleum compounds have been identified as weak inducers for the expression of genes in the AhR pathway, including cyp1a (Knecht et al., 2013; Wincent et al., 2015). Further studies isolating such polar petroleum compounds from fresh and weathered crude oils would be necessary to provide clarity into the effects that such xenobiotics would place upon the AhR pathway. Previous studies have demonstrated that CYP1A activity and induction are sensitive biomarkers capable of predicting latent alteration in the development of cardiac structure in early life stage fish, which are difficult to visualize at the larval stage but significantly reduce growth and survival in mature fish (Donald et al., 2023; Heintz, 2007; Incardona et al., 2015). Our study provides strong evidence that CYP1A activity and induction serve as sensitive biomarkers for early life stage fish, particularly at lower aqueous concentrations of aromatics and naphthenic acids, when developmental abnormalities are not as evident at 7 days post fertilization.

5. Conclusions

This study demonstrated that both DB and CC induce a high hazard risk when spilled into freshwater systems under warm water conditions (24 °C). Even after 56 days of weathering, highly sublethal toxic effects remained that would likely result in latent mortality of developing fish. Notably, the light CC induced lethality only on the first day post oil spill, while the Cold Lake Blend DB induced significantly elevated levels of lethality for 14 days, despite the contaminated waters of the light CC containing consistently higher concentrations of aromatics. Furthermore, our investigation highlights the correlation between classic naphthenic acids and lethal and developmental toxicity endpoints in freshwater contaminated with DB. However, the subsequent impacts of naphthenic acids upon aquatic environments following crude oil spills remain poorly understood. Recent advances in analytical techniques such as Orbitrap MS allow for more precise understanding of the toxic polar organic compounds present in the UCM and should be applied in future studies. Further research into the influence of naphthenic acids and other polar organics is warranted to comprehensively assess the risks posed by both conventional and unconventional crude oils to aquatic ecosystems.

Declaration of competing interest

The authors declare that they have no known competing financial interests or personal relationships that could have appeared to influence the work reported in this paper.

Data availability

Data will be made available on request.

Acknowledgements

The authors acknowledge the funding from the Natural Resources Canada (NRCan) to HD and VSL, the Canada Research Chair Program to VSL, and from the Lake Huron Coastal Centre to SH.

Author contributions

Scott Hepditch contributed to the main writing, experimental design, performing the exposures, sample preparation, sample analysis, data analysis.

Juan Manual Gutierrez Villagomez contributed to the experimental design, performing the exposures, sample preparation, sample analysis, data analysis.

Tuan Anh To contributed to performing the exposures, sample analysis, data analysis, reviewing.

Ève Larocque contributed to sample preparation, sample analysis, data analysis.

Xin Qin to experimental design, DB and CC oil sample preparation, sample analysis, data analysis, reviewing.

Nicole Heshka sample analysis, data analysis, reviewing.

Heather Dettman contributed to experimental design, funding acquisition, reviewing.

Gaëlle Triffault-Bouchet contributed to funding acquisition, sample analysis, reviewing.

Jason Ahad contributed to DB and CC oil sample analysis, funding acquisition, reviewing.

Valerie S. Langlois contributed to the experimental design, funding acquisition, supervision, reviewing.

Data availability.

Data are available upon request.

Appendix A. Supplementary data

Supplementary data to this article can be found online at https://doi.org/10.1016/j.envint.2024.108944.

References

Ahad, J.M.E., Pakdel, H., Gammon, P.R., Siddique, T., Kuznetsova, A., Savard, M.M., 2018. Evaluating in situ biodegradation of 13C-labelled naphthenic acids in groundwater near oil sands tailings ponds. Sci. Total Environ. 643, 392–399. https://doi.org/10.1016/j.scitotenv.2018.06.159.

Alsaadi, F., Madison, B.N., Brown, R.S., Hodson, P.V., Langlois, V.S., 2018. Morphological and molecular effects of two diluted bitumens on developing fathead minnow (Pimephales promelas). Aquat. Toxicol. 204 (September), 107–116. https://doi.org/10.1016/j.aquatox.2018.09.003.

An, D., Brown, D., Chatterjee, I., Dong, X., Ramos-Padron, E., Wilson, S., Bordenave, S., Caffrey, S.M., Gieg, L.M., Sensen, C.W., Voordouw, G., 2013. Microbial community and potential functional gene diversity involved in anaerobic hydrocarbon degradation and methanogenesis in an oil sands tailings pond. Genome 56 (10), 612–618. https://doi.org/10.1139/GEN-2013-0083/SUPPL_FILE/GEN-2013-0083SUPPLA.DOCX.

Aranda, P.S., LaJoie, D.M., Jorcyk, C.L., 2012. Bleach gel: A simple agarose gel for analyzing RNA quality. Electrophoresis 33, 366–369. https://doi.org/10.1002/elps.201100335.

ASTM, 2009. D7573 - 09 - Standard Test Method for Total Carbon and Organic Carbon in Water by High Temperature Catalytic Combustion and Infrared Detection.

ASTM, 2016. D7169-11 - Standard Test Method for Boiling Point Distribution of Samples with Residues Such as Crude Oils and Atmospheric and Vacuum Residues by High Temperature Gas Chromatography.

BCME, 2007. Ambient Water Quality Guidelines for Xylene.

Bekins, B.A., Brennan, J.C., Tillitt, D.E., Cozzarelli, I.M., Illig, J.M.G., Martinović-Weigelt, D., 2020. Biological Effects of Hydrocarbon Degradation Intermediates: Is the Total Petroleum Hydrocarbon Analytical Method Adequate for Risk Assessment? Environ. Sci. Tech. 54 (18), 11396–11404. https://doi.org/10.1021/acs.est.0c02220.

Bérubé, R., Gauthier, C., Bourdin, T., Bouffard, M., Triffault-Bouchet, G., Langlois, V.S., Couture, P., 2021. Lethal and sublethal effects of diluted bitumen and conventional oil on fathead minnow (Pimephales promelas) larvae exposed during their early development. Aquat. Toxicol. 237, 105884 https://doi.org/10.1016/j.aquatox.2021.105884.

Bérubé, R., Garnier, C., Lefebvre-Raine, M., Gauthier, C., Bergeron, N., Triffault-Bouchet, G., Langlois, V.S., Couture, P., 2023. Early developmental toxicity of Atlantic salmon exposed to conventional and unconventional oils. Ecotoxicol. Environ. Saf. 250, 114487 https://doi.org/10.1016/j.ecoenv.2022.114487.

Brette, F., Shiels, H.A., Galli, G.L.J., Cros, C., Incardona, J.P., Scholz, N.L., Block, B.A., 2017. A Novel Cardiotoxic Mechanism for a Pervasive Global Pollutant. Sci. Rep. 7 (1), 41476. https://doi.org/10.1038/srep41476.

Carls, M.G., Holland, L., Larsen, M., Collier, T.K., Scholz, N.L., Incardona, J.P., 2008. Fish embryos are damaged by dissolved PAHs, not oil particles. Aquat. Toxicol. 88 (2), 121–127. https://doi.org/10.1016/J.AQUATOX.2008.03.014.

CCME, 1999a. Canadian water quality guidelines for the protection of aquatic life: Benzene. In Canadian Council of Ministers of the Environment, Canadian environmental quality guidelines. Canadian Council of Ministers of the Environment.

CCME, 1999c. Canadian water quality guidelines for the protection of aquatic life: Toluene. In Canadian Council of Ministers of the Environment, Canadian environmental quality guidelines. Canadian Council of Ministers of the Environment.

CCME, 1999b. Canadian water quality guidelines for the protection of aquatic life: Ethylbenzene. In Canadian Council of Ministers of the Environment, Canadian environmental quality guidelines. Canadian Council of Ministers of the Environment.

CEAEQ, 2015. Détermination Des Composés Organiques Volatils Dans L'eau et Les Sols : Dosage Par « Purge and Trap » Couplé à Un Chromatographe En Phase Gazeuse et à Un Spectromètre De Masse Vol. 03, Issue révision 4.

CEAEQ, 2016. Détermination Des Hydrocarbures Aromatiques Polycycliques : Dosage Par Chromatographie En Phase Gazeuse Couplée à Un Spectromètre De Masse Vol. MA, 400. Issue révision 5.

CEAEQ, 2016. Détermination Des Hydrocarbures Pétroliers (C10 à C50): Dosage Par Chromatographie En Phase Gazeuse Couplée à Un Détecteur à Ionisation De Flamme Vol. MA. 400 – (Issue révision 3).

CER, 2022. Market Snapshot: Bitumen Production Hits a Record High in 2021. Canadian Energy Regulator. https://www.cer-rec.gc.ca/en/data-analysis/energy-markets/market-snapshots/2022/market-snapshot-bitumen-production-hits-record-high-2021.html?fbclid=IwAR0d_IMxavvsmS2Y9NRs6m_hg6UkkVwsYbMEhI--krpu9k3hm-EWXpPoNQ&wbdisable=true.

Cherr, G.N., Fairbairn, E., Whitehead, A., 2017. Impacts of Petroleum-Derived Pollutants on Fish Development 5, 185–203. https://doi.org/10.1146/Annurev-Animal-022516-022928.

Cho, Y., Na, J.G., Nho, N.S., Kim, S., Kim, S., 2012. Application of saturates, aromatics, resins, and asphaltenes crude oil fractionation for detailed chemical characterization of heavy crude oils by fourier transform ion cyclotron resonance mass spectrometry equipped with atmospheric pressure photoionization. Energy Fuel 26 (5), 2558–2565. https://doi.org/10.1021/EF201312M/ASSET/IMAGES/LARGE/EF-2011-01312M_0008.JPEG.

Devlin, E. W., Brammer, J. D., Puyear, R. L., & McKim, J., 1996. Prehatching Development of the Fathead Minnow Pimephales Promelas Rafinesq ue.

Di Toro, D.M., McGrath, J.A., Hansen, D.J., 2000. Technical basis for narcotic chemicals and polycyclic aromatic hydrocarbon criteria. I. Water and tissue. Environ. Toxicol. Chem. 19 (8), 1951–1970. https://doi.org/10.1002/etc.5620190803.

Donald, C.E., Sørhus, E., Perrichon, P., Nakken, C.L., Goksøyr, A., Jørgensen, K.B., Mayer, P., da Silva, D.A.M., Meier, S., 2023. Co-Exposure of Phenanthrene and the cyp-Inducer 3-Methylchrysene Leads to Altered Biotransformation and Increased Toxicity in Fish Egg and Larvae. Environ. Sci. Tech. 57 (30), 11022–11031. https://doi.org/10.1021/ACS.EST.3C02770/ASSET/IMAGES/MEDIUM/ES3C02770_0007.GIF.

Escher, B.I., Ashauer, R., Dyer, S., Hermens, J.L.M., Lee, J.H., Leslie, H.A., Mayer, P., Meador, J.P., Warnekk, M.S.J., 2011. Crucial role of mechanisms and modes of toxic action for understanding tissue residue toxicity and internal effect concentrations of organic chemicals. Integr. Environ. Assess. Manag. 7 (1), 28–49. https://doi.org/10.1002/IEAM.100.

Fallahtafti, S., Rantanen, T., Brown, R.S., Snieckus, V., Hodson, P.V., 2012. Toxicity of hydroxylated alkyl-phenanthrenes to the early life stages of Japanese medaka (Oryzias latipes). Aquat. Toxicol. 106–107, 56–64. https://doi.org/10.1016/J.AQUATOX.2011.10.007.

Frank, R.A., Kavanagh, R., Kent Burnison, B., Arsenault, G., Headley, J.V., Peru, K.M., Van Der Kraak, G., Solomon, K.R., 2008. Toxicity assessment of collected fractions from an extracted naphthenic acid mixture. Chemosphere 72 (9), 1309–1314. https://doi.org/10.1016/J.CHEMOSPHERE.2008.04.078.

Frank, R.A., Fischer, K., Kavanagh, R., Kent Burnison, B., Arsenault, G., Headley, J.V., Peru, K.M., Van Glen Kraak, D.E.R., Solomon, K.R., 2009. Effect of carboxylic acid content on the acute toxicity of oil sands naphthenic acids. Environ. Sci. Tech. 43 (2), 266–271. https://doi.org/10.1021/ES8021057/SUPPL_FILE/ES8021057_SI_001.PDF.

Frank, R.A., Sanderson, H., Kavanagh, R., Burnison, B.K., Headley, J.V., Solomon, K.R., 2009. Use of a (Quantitative) Structure-Activity Relationship [(Q)Sar] Model to Predict the Toxicity of Naphthenic Acids. J. Toxic. Environ. Health A 73 (4), 319–329. https://doi.org/10.1080/15287390903421235.

French-McCay, D.P., Parkerton, T.F., de Jourdan, B., 2023. Bridging the lab to field divide: Advancing oil spill biological effects models requires revisiting aquatic toxicity testing. Aquat. Toxicol. 256, 106389 https://doi.org/10.1016/j.aquatox.2022.106389.

Gutierrez-Villagomez, J. M., Edington, C., Headley, J. V, Pauli, B. D., & Trudeau, V. L. (2019). *Naphthenic Acid Mixtures and Acid-Extractable Organics from Oil Sands Process-A ff ected Water Impair Embryonic Development of Silurana (Xenopus) tropicalis*. Doi: 10.1021/acs.est.8b04461.

Gutierrez-Villagomez, J. M., Martyniuk, C. J., Xing, L., Langlois, V. S., Pauli, B. D., Blais, J. M., & Trudeau, V. L. (2019). Transcriptome Analysis Reveals That Naphthenic Acids Perturb Gene Networks Related to Metabolic Processes, Membrane Integrity, and Gut Function in Silurana (Xenopus) tropicalis Embryos . In Frontiers in Marine Science (Vol. 6).

Gutierrez-Villagomez, J.M., Lara-Jacobo, L.R., Gauthier, C., Patey, G., Xin, Q., Triffaut-Bouchet, G., Dettman, H., Langlois, V.S., 2024. Diluted bitumen weathered under warm or cold temperatures is equally toxic in freshwater fish. Front. Environ. Sci. 12, 1328313. https://doi.org/10.3389/FENVS.2024.1328313.

Headley, J.V., Peru, K.M., McMartin, D.W., Winkler, M., 2002. Determination of Dissolved Naphthenic Acids in Natural Waters by Using Negative-Ion Electrospray Mass Spectrometry. J. AOAC Int. 85 (1), 182–187. https://doi.org/10.1093/JAOAC/85.1.182.

Headley, J.V., Peru, K.M., Janfada, A., Fahlman, B., Gu, C., Hassan, S., 2011. Characterization of oil sands acids in plant tissue using Orbitrap ultra-high resolution mass spectrometry with electrospray ionization. Rapid Commun. Mass Spectrom. 25 (3), 459–462. https://doi.org/10.1002/RCM.4877.

Headley, J.V., Peru, K.M., Fahlman, B., Colodey, A., McMartin, D.W., 2013. Selective solvent extraction and characterization of the acid extractable fraction of Athabasca oils sands process waters by Orbitrap mass spectrometry. Int. J. Mass Spectrom. 345–347, 104–108. https://doi.org/10.1016/J.IJMS.2012.08.023.

Hein, F.J., 2017. Geology of bitumen and heavy oil: An overview. J. Pet. Sci. Eng. 154, 551–563. https://doi.org/10.1016/j.petrol.2016.11.025.

Heintz, R.A., 2007. Chronic exposure to polynuclear aromatic hydrocarbons in natal habitats leads to decreased equilibrium size, growth, and stability of pink salmon populations. Integr. Environ. Assess. Manag. 3 (3), 351–363. https://doi.org/10.1002/IEAM.5630030306.

Hepditch, S.L.J., Ahad, J.M.E., Martel, R., To, T.A., Gutierrez-Villagomez, J.M., Larocque, È., Vander Meulen, I.J., Headley, J.V., Xin, Q., Langlois, V., 2024. Behavior and Fate of Spilled Diluted Bitumen and Conventional Heavy Crude Oil in Shallow Groundwater Systems. In Preparation. https://doi.org/10.2139/SSRN.4726089.

Heshka, N.E., Peru, K.M., Xin, Q., Dettman, H.D., Headley, J.V., 2022. High resolution Orbitrap mass spectrometry analysis of oxidized hydrocarbons found in freshwater following a simulated spill of crude oil. Chemosphere 292. https://doi.org/10.1016/j.chemosphere.2021.133415.

Hodson, P.V., 2017. The Toxicity to Fish Embryos of PAH in Crude and Refined Oils. Arch. Environ. Contam. Toxicol. 73 (1), 12–18. https://doi.org/10.1007/s00244-016-0357-6.

Hounjet, L.J., Xin, Q., McDonald, R., 2023. Bitumen processing reduces diluent content of pipeline-transportable products and can mitigate impacts of spills into various water types. Fuel 331, 125826. https://doi.org/10.1016/j.fuel.2022.125826.

Hughes, S.A., Mahaffey, A., Shore, B., Baker, J., Kilgour, B., Brown, C., Peru, K.M., Headley, J.V., Bailey, H.C., 2017. Using ultrahigh-resolution mass spectrometry and toxicity identification techniques to characterize the toxicity of oil sands process-affected water: The case for classical naphthenic acids. Environ. Toxicol. Chem. 36 (11), 3148–3157. https://doi.org/10.1002/etc.3892.

Incardona, J.P., 2017. Molecular Mechanisms of Crude Oil Developmental Toxicity in Fish. Arch. Environ. Contam. Toxicol. 73 (1), 19–32. https://doi.org/10.1007/s00244-017-0381-1.

Incardona, J.P., Scholz, N.L., 2017. Environmental Pollution and the Fish Heart. Fish Physiology 36 (PartB), 373–433. https://doi.org/10.1016/BS.FP.2017.09.006.

Incardona, J.P., Collier, T.K., Scholz, N.L., 2004. Defects in Cardiac Function Precede Morphological Abnormalities in Fish Embryos Exposed to Polycyclic Aromatic Hydrocarbons. 196, 191–205. https://doi.org/10.1016/j.taap.2003.11.026.

Incardona, J. P., Carls, M. G., Holland, L., Linbo, T. L., Baldwin, D. H., Myers, M. S., Peck, K. A., Tagal, M., Rice, S. D., & Scholz, N. L. (2015). Very low embryonic crude oil exposures cause lasting cardiac defects in salmon and herring. *Scientific Reports 2015 5:1*, *5*(1), 1–13. Doi: 10.1038/srep13499.

Jacobo, L.R.L., Gauthier, C., Xin, Q., Dupont, F., Couture, P., Bouchet, T., Dettman, H.D., Langlois, V.S., 2021. Fate and Fathead Minnow Embryotoxicity of Weathering Crude Oil in a Pilot - Scale Spill Tank. 40 (1), 127–138. https://doi.org/10.1002/etc.4891.

Jivraj, M.N., MacKinnon, M., Fung, B., 1995. Naphthenic acid extraction and quantitative analysis with FT-IR spectroscopy. Syncrude Analytical Manuals.

Johnson, R. J., Charles, †, West, E., Swaih, A. M., Folwell, B. D., Smith, B. E., Steven, ‡, Rowland, J., & Whitby, C. (2011). *Aerobic biotransformation of alkyl branched aromatic alkanoic naphthenic acids via two different pathways by a new isolate of Mycobacteriume mi_2649 872..882*. Doi: 10.1111/j.1462-2920.2011.02649.x.

Kais, B., Ottermanns, R., Scheller, F., Braunbeck, T., 2018. Science of the Total Environment Modi fi cation and quanti fi cation of in vivo EROD live-imaging with zebra fi sh (Danio rerio) embryos to detect both induction and inhibition of CYP1A. Sci. Total Environ. 615, 330–347. https://doi.org/10.1016/j.scitotenv.2017.09.257.

Knecht, A.L., Goodale, B.C., Truong, L., Simonich, M.T., Swanson, A.J., Matzke, M.M., Anderson, K.A., Waters, K.M., Tanguay, R.L., 2013. Comparative developmental toxicity of environmentally relevant oxygenated PAHs. Toxicol. Appl. Pharmacol. 271 (2), 266–275. https://doi.org/10.1016/J.TAAP.2013.05.006.

Lara-Jacobo, L.R., Gauthier, C., Xin, Q., Dupont, F., Couture, P., Bouchet, T., Dettman, H. D., Langlois, V.S., 2021. Fate and Fathead Minnow Embryotoxicity of Weathering Crude Oil in a Pilot-Scale Spill Tank. Environ. Toxicol. Chem. 40 (1), 127–138. https://doi.org/10.1002/etc.4891.

Lebordais, M., Gutierrez-Villagomez, J.M., Gigault, J., Baudrimont, M., Langlois, V.S., 2021. Molecular impacts of dietary exposure to nanoplastics combined with arsenic in Canadian oysters (Crassostrea virginica) and bioaccumulation comparison with Caribbean oysters (Isognomon alatus). Chemosphere 277, 130331. https://doi.org/10.1016/j.chemosphere.2021.130331.

Lee, K., Boufadel, M., Chen, B., Foght, J., Hodson, P., Swanson, S., Venosa, A., 2015. *Expert Panel Report on the Behaviour and Environmental Impacts of Crude Oil Released into Aqueous Environments* (Issue November). Royal Society of Canada.

Li, C., Fu, L., Stafford, J., Belosevic, M., El-din, M.G., 2017. The toxicity of oil sands process-affected water (OSPW): A critical review. Sci. Total Environ. 601–602, 1785–1802. https://doi.org/10.1016/j.scitotenv.2017.06.024.

Marentette, J.R., Chiorean, S., Lavalle, C., Sullivan, C., Parrott, J.L., 2014. Selecting Optimal Eggs and Embryonic Developmental Stages of Fathead Minnow (Pimephales promelas) for Early Life-Stage Toxicity Tests. Arch. Environ. Contam. Toxicol. 66 (2), 227–236. https://doi.org/10.1007/s00244-013-9973-6.

Marentette, J.R., Frank, R.A., Hewitt, L.M., Gillis, P.L., Bartlett, A.J., Brunswick, P., Shang, D., Parrott, J.L., 2015. Sensitivity of walleye (Sander vitreus) and fathead minnow (Pimephales promelas) early-life stages to naphthenic acid fraction components extracted from fresh oil sands process-affected waters. Environ. Pollut. 207, 59–67. https://doi.org/10.1016/j.envpol.2015.08.022.

Mccarrick, S., Cunha, V., Vondr, J., Dreij, K., 2019. In Vitro and in Vivo Genotoxicity of Oxygenated Polycyclic Aromatic. 246, 678–687. https://doi.org/10.1016/j.envpol.2018.12.092.

McGrath, J.A., Di Toro, D.M., 2009. Validation of the target lipid model for toxicity assessment of residual petroleum constituents: Monocyclic and polycyclic aromatic hydrocarbons. Environ. Toxicol. Chem. 28 (6), 1130–1148. https://doi.org/10.1897/08-271.1.

Mcgrath, J.A., Fanelli, C.J., Toro, M.D., Parkerton, T.F., Redman, A.D., Paumen, M.L., Comber, M., Eadsforth, C.V., Haan, K.D., 2018. Re-evaluation of Target Lipid Model – Derived HC5 Predictions for. Hydrocarbons. 37 (6), 1579–1593. https://doi.org/10.1002/etc.4100.

Meador, J.P., Nahrgang, J., 2019. Characterizing Crude Oil Toxicity to Early-Life Stage Fish Based On a Complex Mixture : Are We Making Unsupported Assumptions? Environ. Sci. Tech. https://doi.org/10.1021/acs.est.9b02889.

Melbye, A.G., Brakstad, O.G., Hokstad, J.N., Gregersen, I.K., Hansen, B.H., Booth, A.M., Rowland, S.J., Tollefsen, K.E., 2009. Chemical and Toxicological Characterization of an Unresolved Complex Mixture-Rich Biodegraded Crude Oil. Environ. Toxicol. Chem. 28 (9), 1815. https://doi.org/10.1897/08-545.1.

Mindorff, L.M., Mahmoudi, N., Hepditch, S.L.J., Langlois, V.S., Alam, S., Martel, R., Ahad, J.M.E., 2023. Isotopic and microbial evidence for biodegradation of diluted bitumen in the unsaturated zone. Environ. Pollut. 322, 121170 https://doi.org/10.1016/j.envpol.2023.121170.

Monaghan, J., Richards, L.C., Vandergrift, G.W., Hounjet, L.J., Stoyanov, S.R., Gill, C.G., Krogh, E.T., 2021. Direct mass spectrometric analysis of naphthenic acids and polycyclic aromatic hydrocarbons in waters impacted by diluted bitumen and conventional crude oil. Sci. Total Environ. 765, 144206 https://doi.org/10.1016/J.SCITOTENV.2020.144206.

Monaghan, J., Xin, Q., Aplin, R., Jaeger, A., Heshka, N.E., Hounjet, L.J., Gill, C.G., Krogh, E.T., 2022. Aqueous naphthenic acids and polycyclic aromatic hydrocarbons in a meso-scale spill tank affected by diluted bitumen analyzed directly by membrane introduction mass spectrometry. J. Hazard. Mater. 440, 129798 https://doi.org/10.1016/j.jhazmat.2022.129798.

Motulsky, H.J., Brown, R.E., 2006. Detecting outliers when fitting data with nonlinear regression – a new method based on robust nonlinear regression and the false discovery rate. BMC Bioinf. 7 (1), 123. https://doi.org/10.1186/1471-2105-7-123.

Nasem, 2022. Oil in the Sea IV: Inputs. Fates, and Effects. https://doi.org/10.17226/26410.

Neuwirth, E. (2014). *RColorBrewer: ColorBrewer Palettes*.

NOAA. (2019). *Diluted Bitumen Spills*.

Pathiratne, A., Hemachandra, C.K., 2010. Modulation of ethoxyresorufin O-deethylase and glutathione S-transferase activities in Nile tilapia (Oreochromis niloticus) by polycyclic aromatic hydrocarbons containing two to four rings: Implications in biomonitoring aquatic pollution. Ecotoxicology 19 (6), 1012–1018. https://doi.org/10.1007/S10646-010-0482-3/TABLES/1.

Philibert, D. A., Philibert, C. P., Lewis, C., & Tierney, K. B. (2016). *Comparison of Diluted Bitumen (Dilbit) and Conventional Crude Oil Toxicity to Developing Zebra fi sh*. Doi: 10.1021/acs.est.6b00949.

Podgorski, D.C., Bekins, B.A., 2023. Comment on "Complex mixture toxicology: Evaluation of toxicity to freshwater aquatic receptors from biodegradation metabolites in groundwater at a crude oil release site, recent analogous results from other authors, and implications for risk management". Aquat. Toxicol. 265, 106744 https://doi.org/10.1016/J.AQUATOX.2023.106744.

Ripmeester, M.J., Duford, D.A., 2019. Method for routine "naphthenic acids fraction compounds" determination in oil sands process-affected water by liquid-liquid extraction in dichloromethane and Fourier-Transform Infrared Spectroscopy. Chemosphere 233, 687–696. https://doi.org/10.1016/J.CHEMOSPHERE.2019.05.222.

Roex, E.W.M., Van Gestel, C.A.M., Van Wezel, A.P., Van Straalen, N.M., 2000. Ratios between acute aquatic toxicity and effects on population growth rates in relation to toxicant mode of action. Environ. Toxicol. Chem. 19 (3), 685–693. https://doi.org/10.1002/ETC.5620190321.

Rogers, V.V., Liber, K., MacKinnon, M.D., 2002. Isolation and characterization of naphthenic acids from Athabasca oil sands tailings pond water. Chemosphere 48 (5), 519–527. https://doi.org/10.1016/S0045-6535(02)00133-9.

Saborimanesh, N., Xin, Q., Ridenour, C., Farooqi, H., 2023. Response of microbial communities in North Saskatchewan River to diluted bitumen and conventional crude under freeze-thaw-refreeze cycle. Environ. Pollut. 323, 121256 https://doi.org/10.1016/J.ENVPOL.2023.121256.

Scholz, S., Schreiber, R., Armitage, J., Mayer, P., Escher, B.I., Lidzba, A., Léonard, M., Altenburger, R., 2018. Meta-analysis of fish early life stage tests—Association of toxic ratios and acute-to-chronic ratios with modes of action. Environ. Toxicol. Chem. 37 (4), 955–969. https://doi.org/10.1002/ETC.4090.

Schrlau, J.E., Kramer, A.L., Chlebowski, A., Truong, L., Tanguay, R.L., Simonich, S.L.M., Semprini, L., 2017. Formation of Developmentally Toxic Phenanthrene Metabolite Mixtures by Mycobacterium sp. ELW1. Environ. Sci. Tech. 51 (15), 8569–8578. https://doi.org/10.1021/ACS.EST.7B01377/SUPPL_FILE/ES7B01377_SI_001.PDF.

Shailaja, M.S., D'Silva, C., 2003. Evaluation of impact of PAH on a tropical fish, Oreochromis mossambicus using multiple biomarkers. Chemosphere 53 (8), 835–841. https://doi.org/10.1016/S0045-6535(03)00667-2.

Sørensen, L., Meier, S., Mjøs, S.A., 2016. Application of gas chromatography/tandem mass spectrometry to determine a wide range of petrogenic alkylated polycyclic aromatic hydrocarbons in biotic samples. Rapid Commun. Mass Spectrom. 30 (18), 2052–2058. https://doi.org/10.1002/RCM.7688.

Speight, J.G., 2019. Handbook of industrial hydrocarbon processes. Gulf Professional Publishing.

Stoyanovich, S., Rodríguez-Gil, J.R., Hanson, M.L., Hollebone, B.P., Orihel, D.M., Palace, V.P., Faragher, R., Mirnaghi, F.S., Shah, K., Yang, Z., Blais, J.M., 2021. Simulating diluted bitumen spills in boreal lake limnocorrals - part 2: Factors affecting the physical characteristics and submergence of diluted bitumen. Sci. Total Environ. 790, 148580 https://doi.org/10.1016/j.scitotenv.2021.148580.

Sutton, P.A., Lewis, C.A., Rowland, S.J., 2005. Isolation of individual hydrocarbons from the unresolved complex hydrocarbon mixture of a biodegraded crude oil using preparative capillary gas chromatography. Org Geochem. 36 (6), 963–970. https://doi.org/10.1016/J.ORGGEOCHEM.2004.11.007.

USEPA. (2002). *Short-term Methods for Estimating the Chronic Toxicity of Effluents and Receiving Waters to Freshwater Organisms* (Issue October).

Wincent, E., Jönsson, M.E., Bottai, M., Lundstedt, S., Dreij, K., 2015. Aryl hydrocarbon receptor activation and developmental toxicity in zebrafish in response to soil extracts containing unsubstituted and oxygenated pahs. Environ. Sci. Tech. 49 (6), 3869–3877. https://doi.org/10.1021/ES505588S/SUPPL_FILE/ES505588S_SI_001.PDF.

Xin, Q., Saborimanesh, N., Greer, C.W., Farooqi, H., Dettman, H.D., 2023. The effect of temperature on hydrocarbon profiles and the microbial community composition in North Saskatchewan River water during mesoscale tank tests of diluted bitumen spills. Sci. Total Environ. 859, 160161 https://doi.org/10.1016/j.scitotenv.2022.160161.

Xin, Q., Saborimanesh, N., Ridenour, C., Farooqi, H., 2024. Fate, behaviour and microbial response of diluted bitumen and conventional crude spills in a simulated warm freshwater environment. Environ. Pollut. 343, 123224 https://doi.org/10.1016/j.envpol.2023.123224.

Zhang, L., Zhang, Y., Gamal El-Din, M., 2018. Degradation of Recalcitrant Naphthenic Acids from Raw and Ozonated Oil Sands Process-Affected Waters by a Semi-Passive Biofiltration Process. https://doi.org/10.1016/j.watres.2018.01.001.